

Serveur Académique Lausannois SERVAL serval.unil.ch

Author Manuscript

Faculty of Biology and Medicine Publication

This paper has been peer-reviewed but does not include the final publisher proof-corrections or journal pagination.

Published in final edited form as:

Title: Hyperpolarized (6) Li as a probe for hemoglobin oxygenation level.

Authors: Balzan R, Mishkovsky M, Simonenko Y, van Heeswijk RB, Gruetter R, Eliav U, Navon G, Comment A

Journal: Contrast media & molecular imaging

Year: 2016 Jan

Volume: 11

Issue: 1

Pages: 41-6

DOI: 10.1002/cmami.1656

Hyperpolarized ^6Li as a probe for hemoglobin oxygenation level

Riccardo Balzan^{1‡}, Mor Mishkovsky^{2,3*‡}, Yana Solomon⁴, Ruud B. van Heeswijk³,
Rolf Gruetter^{2,3,5}, Uzi Eliav⁴, Gil Navon⁴, Arnaud Comment¹

¹*Institute of Physics of Biological Systems, Ecole Polytechnique Fédérale de Lausanne, CH-1015 Lausanne, Switzerland*

²*Laboratory for Functional and Metabolic Imaging, Ecole Polytechnique Fédérale de Lausanne, CH-1015 Lausanne, Switzerland*

³*Department of Radiology, Université de Lausanne, CH-1015 Lausanne, Switzerland*

⁴*School of Chemistry, Tel-Aviv University, Ramat-Aviv, Tel Aviv, Israel*

⁵*Department of Radiology, Geneva University Hospital and Faculty of Medicine, University of Geneva, CH-1211 Genève 4, Switzerland.*

*Correspondence:

mor.mishkovsky@epfl.ch

‡ R.B. and M.M. contributed equally to this work

Keywords: Lithium, Hyperpolarization, Dynamic Nuclear Polarization, Magnetic Resonance, MRI, Molecular Imaging, Blood, Deoxyhemoglobin.

ABSTRACT

Hyperpolarization by dissolution dynamic nuclear polarization (DNP) is a versatile technique to dramatically enhance the nuclear magnetic resonance (NMR) signal intensity of insensitive long- T_1 nuclear spins such as ${}^6\text{Li}$. The ${}^6\text{Li}$ longitudinal relaxation of lithium ions in aqueous solutions highly depends on the concentration of paramagnetic species, even if they are present in minute amounts. We herein demonstrate that blood oxygenation can be readily detected by taking advantage of the ${}^6\text{Li}$ signal enhancement provided by dissolution DNP together with the more than 10% decrease in ${}^6\text{Li}$ longitudinal relaxation as a consequence of the presence of paramagnetic deoxyhemoglobin.

INTRODUCTION

Oxygen delivery and consumption correlate with the physiological state of tissues and organs and affect their metabolism. Pathological situations are characterized by variations in oxygenation levels (1,2), which may directly affect treatment and recovery (3,4). Oxygen uptake can be measured by positron emission tomography (PET) imaging following the inhalation of ${}^{15}\text{O}_2$. However the short ${}^{15}\text{O}$ half-life (2.1 min) limits its availability as it requires the need of an onsite cyclotron, and the use of ionizing radiation restricts the number of examinations per patient (5). Alternatively, the stable ${}^{17}\text{O}$ isotope can be used to probe oxygen metabolism by magnetic resonance (MR). Unlike ${}^{15}\text{O}$ PET, ${}^{17}\text{O}$ MR offers the advantage to selectively measure the metabolically generated $\text{H}_2{}^{17}\text{O}$ without confounding signals from the ${}^{17}\text{O}_2$ molecules bound to hemoglobin. However, the low gyromagnetic ratio of ${}^{17}\text{O}$ (5.77 MHz/T) and the short associated T_2^* relaxation time (~ 2 ms) leads to low sensitivity (6). A different MR method for mapping oxygenation level is based on the blood oxygenation level dependent (BOLD) contrast which relies on the effect of paramagnetic deoxyhemoglobin on proton transverse relaxation (7). Although BOLD MR imaging is mostly known in the context of cognitive neuroscience as functional

MRI, recent studies have shown that it can be used to map hypoxic regions in tumors (8). The major drawback of this T_2^* -weighted imaging approach lies in the dependence of T_2^* on many other parameters other than the oxygen level, including magnetic field inhomogeneities, water diffusion, and the structure of the blood vessel network including blood volume, which may represent confounding variables (9).

The recently developed dissolution dynamic nuclear polarization (DNP) technique enables hyperpolarizing nuclear spins of molecules in solutions that can be injected into cell suspensions, perfused organs, animals or humans (10). The large signal resulting from the dramatic increase in polarization allows detecting in real time the biodistribution and the metabolism of molecules containing nuclear spins with long longitudinal relaxation times (11-13). Consequently, DNP-enhanced MR studies have been so far mostly restricted to precursors with non-protonated spin- $\frac{1}{2}$ nuclei such as ^{13}C -labeled carbonyls or ^{15}N -labeled quaternary amines. However, it has been shown that ^6Li , a spin-1 nucleus with an exceptionally small quadrupole moment ($Q < 8.5$ kHz), can also be hyperpolarized using dissolution DNP and that hyperpolarized ^6Li can be detected *in vivo* in the rat brain (14). The ^6Li longitudinal relaxation time of Li^+ ions can be as long as 550 s when dissolved in deoxygenated deuterated water (D_2O) at room temperature (15).

A recent study showed that, following the intraperitoneal administration of lithium to rodents, a large fraction of the Li^+ ions incorporated into the brain is located in the intracellular compartment (16). Hyperpolarized ^6Li could therefore be an interesting contrast media for perfusion imaging with similar methods than the ones proposed with hyperpolarized xenon (17), and hyperpolarized ^{13}C tert-butanol (18). More generally, the potential of hyperpolarized ^6Li as contrast agent for molecular imaging is high because Li^+ ions can replace the ubiquitous and essential Na^+ ions in many biological systems. It was previously shown that the ^6Li T_1 of Li^+ ions in solutions is remarkably sensitive to the presence of paramagnetic species and that hyperpolarized

${}^6\text{Li}$ could be used as a sensor for traces amount ($< \text{mM}$) of Gd-based MR contrast agents (14). The aim of the present study was to detect blood oxygenation level in human and rat blood and plasma using hyperpolarized ${}^6\text{Li}$.

RESULTS

To determine the effect of hemoglobin oxygenation on the T_1 of ${}^6\text{Li}$, we simultaneously measured the decay of the hyperpolarized ${}^6\text{Li}$ signal in three separated tubes, two of them (tubes #1 and #3) containing either whole blood and deoxygenated blood or plasma and deoxygenated plasma, and the third one (tube #2) containing D_2O (99.6% D) to obtain a reference relaxation measurement (Fig. 1). To separate the signal originating from each one of the three tubes, one-dimensional projections (gradient echo) were acquired following non-selective 10° flip angle pulses applied every 20 s. Gradient strength was adjusted to maximize the signal per voxel while avoiding overlap between the signal originating from the three different tubes in the one-dimensional projection. In all measurements, the persistent radical which is necessary for the DNP process was scavenged with sodium ascorbate prior to the infusion of the hyperpolarized solution into the tubes (19). The ${}^6\text{Li}$ decay curves were obtained from each experiment by plotting the magnitude of the signal corresponding to each tube as a function of time (Fig. 2). The characteristic decay constants were obtained by fitting the curves with mono-exponential functions. The longitudinal relaxation time T_1 was deduced after correcting for the effect of the pulses on the signal decay. The ${}^6\text{Li}$ T_1 values measured in blood and plasma samples are presented in Table 1.

To evaluate the effect of the radical scavenger on ${}^6\text{Li}$ T_1 , measurements were performed in thermally polarized 0.5 M ${}^6\text{LiCl}$ aqueous solutions (D_2O , 99.6% D) with or without scavenger (Table 2). The T_1 in pure non-deoxygenated D_2O (99.98 % D) was similar to the previously reported value for deoxygenated D_2O (15). Adding 20 mM of sodium ascorbate, either in its protonated or deuterated form, led to a decrease

in T_1 of about 20 %. Although the exchangeable protons of ascorbate increase the concentration of protonated water molecules and therefore participate in increasing the solvent-induced dipolar relaxation of ${}^6\text{Li}$ (20), the fact that the T_1 was nearly identical when ascorbate was deuterated shows that the most prominent relaxation mechanism induced by the presence of ascorbate is rather due to a direct interaction between Li^+ ions and ascorbate (a complete analysis of the relaxation mechanism is however beyond the scope of the present study). When performing hyperpolarized ${}^6\text{Li}$ MR experiments, it was observed that an ascorbate-to-radical ratio of 3 was insufficient to rapidly scavenge the 0.4 mM of nitroxyl radical present in the final solution since a substantially shorter T_1 was recorded (Table 2). In a second series of experiments performed with a drastically lower radical concentration corresponding to an ascorbate-to-radical ratio of 30 for an ascorbate concentration of 0.45 mM, the contribution of nitroxyl radicals to the ${}^6\text{Li}$ relaxation was effectively quenched and essentially negligible.

Two parameters were measured to assess the efficiency of the deoxygenation procedure: the partial pressure of oxygen (PO_2), representative of the concentration free oxygen gas dissolved in the sample, as well as the oxygen saturation (SO_2), indicating the fraction of hemoglobin bound to oxygen. The relative decrease in PO_2 following deoxygenation, namely $([\text{PO}_2]^{\text{oxy}} - [\text{PO}_2]^{\text{deoxy}}) / [\text{PO}_2]^{\text{oxy}}$, was 5.2% in blood and 36% in plasma, and a relative reduction of $([\text{SO}_2]^{\text{oxy}} - [\text{SO}_2]^{\text{deoxy}}) / [\text{SO}_2]^{\text{oxy}} = 2\%$ was measured in blood (Table 3).

The relative change in ${}^6\text{Li}$ longitudinal relaxation time following deoxygenation, namely $(T_1^{\text{oxy}} - T_1^{\text{deoxy}}) / T_1^{\text{oxy}}$, was computed for each experiment (Fig. 3). We observed in all experiments that the ${}^6\text{Li}$ T_1 is shorter in deoxygenated blood than in whole blood, i.e., partially oxygenated blood, with a mean relative variation between 10 and 15%. Conversely, the observed ${}^6\text{Li}$ T_1 is longer in deoxygenated plasma than in partially oxygenated plasma. To confirm these results at pharmacologically relevant lithium level in anticipation of future *in vivo* studies, a series of experiment

was carried out in rat blood and plasma using deuterated phosphate buffer instead of D₂O for dissolution. The same trend was observed with a relative change of + 10.5 % in rat blood and -6.5% in the plasma following deoxygenation. In this second series of experiments, the standard deviation on the relative differences was significantly lower (less than 10%).

DISCUSSION

The present study shows that hemoglobin oxygenation can be monitored through its influence on the hyperpolarized ⁶Li longitudinal relaxation time. We chose to add ascorbate in the hyperpolarized ⁶Li solutions not only to reduce the detrimental effect of the TEMPOL (4-hydroxy-2,2,6,6-tetramethylpiperidine-1-oxyl) radicals on the relaxation and therefore increase the T₁, but also to improve the reproducibility of the experiments since even slight changes in radical concentration can have a strong effect on the long ⁶Li relaxation time. As was already observed with hyperpolarized [1-¹³C]acetate (20), a relatively large ascorbate-to-radical concentration ratio must be used to completely quench the radicals within the short hyperpolarized MR experiments. However, increasing the scavenger concentration above a certain threshold will also lead to increased relaxation induced by the presence of ascorbate molecules. A possible way to avoid this issue would be to use radicals such as BDPA (1,3-bisdiphenylene-2-phenylallyl), which can be easily filtered out since they precipitate in aqueous solutions (21).

Oxygenated hemoglobin being diamagnetic, it does not affect the ⁶Li relaxation. By blowing argon gas on whole blood samples, oxyhemoglobin was transformed into deoxyhemoglobin. The shorter ⁶Li T₁ observed in deoxygenated blood as compared to non-deoxygenated blood was ascribed to paramagnetic deoxyhemoglobin. The relative $(T_1^{\text{oxy}} - T_1^{\text{deoxy}}) / T_1^{\text{oxy}}$ ratio in ⁶Li longitudinal relaxation time are therefore positive in blood samples (Fig. 3). This effect is similar to the BOLD contrast which originates from the change in proton T₂^{*} induced by the paramagnetic relaxation

caused by the presence of deoxyhemoglobin. In contrast, in plasma, oxygen is present as molecular O_2 which is paramagnetic. Blowing argon removes O_2 thereby reducing the concentration of paramagnetic species from the plasma and leading to increased ${}^6\text{Li}$ T_1 values. The relative $(T_1^{\text{oxy}} - T_1^{\text{deoxy}}) / T_1^{\text{oxy}}$ ratio is therefore negative in plasma (Fig. 3).

A non-negligible variability in the ${}^6\text{Li}$ T_1 values measured in blood and plasma samples was observed, in particular in experiments performed in the first series of experiments (Table 1). These variances were dramatically reduced in the second series of experiments performed with pharmacological doses of lithium and substantially longer T_1 values were recorded in the plasma samples. These two observations led us to conclude once more that a large scavenger-to-radical is necessary to limit the effect of the unavoidable slight variations in radical concentration on T_1 and, while in blood samples the contribution of deoxyhemoglobin to the ${}^6\text{Li}$ longitudinal relaxation is dominant, the nitroxyl radicals seem to be a non-negligible relaxation mechanism in plasma samples.

It also appear that the mean relative $(T_1^{\text{oxy}} - T_1^{\text{deoxy}}) / T_1^{\text{oxy}}$ ratio measure in blood samples is rather similar in all experiments, ranging from 10.5 to 15%, whereas it varies from -6.5 to -20.5% in the plasma samples. This can be explained by the strikingly high variability in plasma PO_2 following the deoxygenation procedure even within the same series of experiments (see Table 3). In addition, the blood and plasma samples used in the second series were more diluted than in the first series of experiments following the injection of 400uL of hyperpolarized ${}^6\text{Li}$ in 1.5 mL of samples instead of 300uL of hyperpolarized ${}^6\text{Li}$ in 2 mL samples (see Experimental section). The oxygen concentration was therefore expected to be higher in the first series of experiments, meaning that a stronger effect of plasma deoxygenation could be expected.

When comparing the relative changes in T_1 measured in the second series of experiments with the results of the gas analyses, it appears that a 2% variation in blood oxygen level translate into a 10.5% change in ${}^6\text{Li}$ T_1 , demonstrating the high sensitivity of the proposed method. Note that a relative variation of 36% in PO_2 measured in plasma only corresponds to a 6.5% change in T_1 , showing that the relaxation of ${}^6\text{Li}$ is remarkably more sensitive to the presence of deoxyhemoglobin than of molecular oxygen.

In a medical context, the primary use of lithium salts is to treat manic-depressive (bipolar) and depressive disorders (22,23). They have been administrated at doses up to 1200 mg/day, which led to serum concentration between 0.3-1 mM (24), a range which is similar to the concentration obtained after infusion of hyperpolarized [1- ${}^{13}\text{C}$]pyruvate in the first clinical study (25). We show that blood oxygenation can be monitored through its influence on the hyperpolarized ${}^6\text{Li}$ longitudinal relaxation time also when using pharmacological lithium doses. The observed difference in T_1 between whole and deoxygenated blood could therefore be possibly used to detect hemoglobin oxygenation level *in vivo*. Due to the ability of Li^+ ions to diffuse freely across cell membranes, T_1 -weighted ${}^6\text{Li}$ imaging could be considered to obtain oxygenation maps. This would be a particularly interesting diagnostic tool for assessing tumor oxygenation level, for instance prior to radiation therapy. It must, however, be borne in mind that the intracellular and extracellular ${}^6\text{Li}$ T_1 might be substantially different and the interpretation of the results could intricate.

EXPERIMENTAL

Fresh human venous blood samples were provided by healthy volunteers. Rat venous blood samples were collected by bleeding 10 male Sprague-Dawley rats (384 ± 40 g). Rats were anesthetized with 1.5% isoflurane in a 30% O_2 /70% N_2O mixture. All animal experiments were performed according to Federal and local ethical guidelines, and the protocols were approved by the local regulatory body (Service de la

consommation et des affaires vétérinaires, Affaires vétérinaires, Canton de Vaud, Suisse). 3 UI/mL of heparin (Drossapharm AGSG, Basel, Switzerland) was added to each human and animal blood samples. Samples were kept refrigerated at 5°C in 50 mL Falcon tubes and were used within two days following blood withdrawal. Plasma was extracted from blood samples following natural phase separation in tubes stored in vertical position at 5°C.

MR measurements were carried out on an actively-shielded horizontal 9.4 T / 31 cm animal scanner (Varian/Magnex, Palo Alto, CA, USA) using a custom-designed ^1H / ^6Li probe based on two stacked 40-mm inner diameter coils (machined from a double-sided printed circuit board) surrounding a cylindrical tube holder (Plexiglass) containing three 10-mm diameter glass tubes, two with thin 0.55-mm walls (513-1PS-7, Wilmad, Vineland, NJ, USA) and one with 1.45-mm wall thickness (513-7PPH-7, Wilmad, Vineland, NJ, USA). The geometry of the tube holder was designed so that the horizontal tomographic projection of each of the three tubes is well separated from one another (Fig. 1). In all experiments the tube holder was inserted inside the magnet bore prior to each dissolution DNP experiment. Proton images were acquired to position the tube holder at the magnet isocenter and static field inhomogeneities were corrected by manual shimming. The deoxygenation process consisted in blowing argon gas inside the glass tube containing either blood or plasma for 10 min, about 5 min prior to the dissolution experiment. Heavy noble gas was preferred over nitrogen gas to prevent air from reoxygenating the samples before and during MR acquisitions. Each tube was then covered with a perforated plastic cap. A polytetrafluoroethylene (PTFE) capillary was inserted through the cap to remotely inject the hyperpolarized $^6\text{Li}^+$ solution into the sample.

A first series of experiments was performed in both human and rat blood using a $^6\text{Li}^+$ concentration of 130 mM. A set of three 2-mL samples each inserted in one glass tube were probed: tube #1 and tube #3 contained either whole blood and deoxygenated blood or plasma and deoxygenated plasma. Tube #2 was filled with pure D_2O and

served as reference to assess the relaxation time of each hyperpolarized ${}^6\text{Li}^+$ solution. Prior to each experiment, 350 μL of 15 M ${}^6\text{LiCl}$ solution prepared in 2:1 $\text{D}_2\text{O}/\text{d}_6$ -ethanol (v/v) doped with 40 mM TEMPOL was inserted, in the form of 2-mm diameter frozen beads, inside a custom-designed 7 T polarizer (26). 50 μL of frozen 1 M aqueous sodium ascorbate solution was added inside the sample cup to scavenge the TEMPOL radicals during the dissolution process (19). All chemicals were purchased from Sigma-Aldrich (Buchs, Switzerland). After 1 h of polarization at 1 ± 0.05 K, the samples were rapidly dissolved in 5 mL of superheated D_2O (180°C) and the resulting hyperpolarized ${}^6\text{Li}^+$ solution was collected out of the polarizer by blowing high-pressure helium gas (6 bar) for 3.5 s through the dissolution insert previously described (27). 300 μL of solution was manually and sequentially injected into each 10 mm-tube through a PTFE capillary within 10 s. Data acquisition started 20 s after dissolution. The liquid-state ${}^6\text{Li}$ polarization at the time of measurements was estimated to be $5\pm 0.3\%$ from a comparison between the hyperpolarized and the thermally polarized ${}^6\text{Li}$ signals.

To confirm these observations at pharmacologically relevant Li^+ level, a second series of experiments was performed in rat blood and plasma. For these experiments, tube #1 and tube #3 were filled with 1.5 mL of either whole blood and deoxygenated blood or plasma and deoxygenated plasma. Tube #2 was filled with 1.5 mL of pure D_2O . An amount of 5 μL of 3 M ${}^6\text{LiCl}$ frozen solution prepared in 1:1 $\text{D}_2\text{O}/\text{glycerol-d}_8$ (w/w) doped with 58 mM TEMPOL was inserted inside the polarizer along with 10 μL of frozen 1 M aqueous sodium ascorbate solution. The concentration of lithium salt was reduced from 15 M to 3 M to avoid inaccuracy in sample volume when preparing the frozen beads. Polarization time was set to 1.5 h and the samples were dissolved in 5 mL of superheated deuterated phosphate buffer. The liquid-state ${}^6\text{Li}$ polarization was $7.4\pm 0.5\%$. After having collected the hyperpolarized ${}^6\text{Li}^+$ solution, 400 μL of solution was manually and sequentially injected prior to data acquisition. The other parameters were identical to the ones set in the first series of experiments.

In conjunction with the hyperpolarized ^6Li MR experiments, oxygen gas analysis was performed in samples prepared in the exact same way than those used in the second series of experiments. For these analyses, 100 μL aliquots of blood or plasma were taken from each sample and the PO_2 and SO_2 values were obtained using a COBAS[®] b 121 system (Roche Diagnostic GmbH, Mannheim, Germany).

ACKNOWLEDGMENTS AND COMPETING INTERESTS

We thank Dr. Mario Lepore for his help with animal handling and blood analyses. The authors declare no competing financial interests. This work was supported by the Swiss National Science Foundation (grant 200020_124901 and PP00P2_133562 to A.C. and grant 31003A_131087 to R.G.), the Centre d'Imagerie BioMédicale (CIBM) of the UNIL, UNIGE, HUG, CHUV, EPFL, and the Leenards and Jeantet Foundations.

REFERENCES

1. Ishii K, Kitagaki H, Kono M, Mori E. Decreased medial temporal oxygen metabolism in Alzheimer's disease shown by PET. *Journal of Nuclear Medicine* 1996;37(7):1159-1165.
2. Karimi M, Golchin N, Tabbal SD, Hershey T, Videen TO, Wu J, Usche JWM, Revilla FJ, Hartlein JM, Wernle AR, Mink JW, Perlmutter JS. Subthalamic nucleus stimulation-induced regional blood flow responses correlate with improvement of motor signs in Parkinson disease. *Brain* 2008;131:2710-2719.
3. Brown JM, William WR. Exploiting tumour hypoxia in cancer treatment. *Nat Rev Cancer* 2004;4(6):437-447.
4. Rother J, Schellinger PD, Gass A, Siebler M, Villringer A, Fiebach JB, Fiehler J, Jansen O, Kucinski T, Schoder V, Szabo K, Junge-Hulsing GJ, Hennerici M, Zeumer H, Sartor K, Weiller C, Hacke W, Stu KS. Effect of intravenous thrombolysis on MRI parameters and functional outcome in acute stroke < 6 hours. *Stroke* 2002;33(10):2438-2445.
5. Baron JC, Jones T. Oxygen metabolism, oxygen extraction and positron emission tomography: Historical perspective and impact on basic and clinical neuroscience. *Neuroimage* 2012;61(2):492-504.
6. Gordji-Nejad A, Mollenhoff K, Oros-Peusquens AM, Pillai DR, Shah NJ. Characterizing cerebral oxygen metabolism employing oxygen-17 MRI/MRS at high fields. *Magnetic Resonance Materials in Physics Biology and Medicine* 2014;27(1):81-93.
7. Ogawa S, Lee TM, Kay AR, Tank DW. Brain Magnetic-Resonance-Imaging with Contrast Dependent on Blood Oxygenation. *Proceedings of the National Academy of Sciences of the United States of America* 1990;87(24):9868-9872.
8. Price JM, Robinson SP, Koh DM. Imaging hypoxia in tumours with advanced MRI. *Q J Nucl Med Mol Im* 2013;57(3):257-270.
9. Christen T, Lemasson B, Pannetier N, Farion R, Remy C, Zaharchuk G, Barbier EL. Is T2* Enough to Assess Oxygenation? Quantitative Blood Oxygen Level-Dependent Analysis in Brain Tumor. *Radiology* 2012;262(2):495-502.
10. Ardenkjaer-Larsen JH, Fridlund B, Gram A, Hansson G, Hansson L, Lerche MH, Servin R, Thaning M, Golman K. Increase in signal-to-noise ratio of > 10,000 times in liquid-state NMR. *Proceedings of the National Academy of Sciences of the United States of America* 2003;100(18):10158-10163.
11. Gallagher FA, Kettunen MI, Brindle KM. Biomedical applications of hyperpolarized C-13 magnetic resonance imaging. *Progress in Nuclear Magnetic Resonance Spectroscopy* 2009;55(4):285-295.
12. Golman K, in't Zandt R, Thaning M. Real-time metabolic imaging. *Proceedings of the National Academy of Sciences of the United States of America* 2006;103(30):11270-11275.
13. Kurhanewicz J, Vigneron DB, Brindle K, Chekmenev EY, Comment A, Cunningham CH, DeBerardinis RJ, Green GG, Leach MO, Rajan SS, Rizi RR, Ross BD, Warren WS, Malloy CR. Analysis of Cancer Metabolism by Imaging Hyperpolarized Nuclei: Prospects for Translation to Clinical Research. *Neoplasia* 2011;13(2):81-97.

14. van Heeswijk RB, Uffmann K, Comment A, Kurdzesau F, Perazzolo C, Cudalbu C, Jannin S, Konter JA, Hautle P, van den Brandt B, Navon G, van der Klink JJ, Gruetter R. Hyperpolarized Lithium-6 as a Sensor of Nanomolar Contrast Agents. *Magnetic Resonance in Medicine* 2009;61(6):1489-1493.
15. Wehrli FW. Temperature-Dependent Spin-Lattice Relaxation of Li-6 in Aqueous Lithium-Chloride. *Journal of Magnetic Resonance* 1976;23(3):527-532.
16. Komoroski RA, Lindquist DM, Pearce JM. Lithium compartmentation in brain by (7) Li MRS: effect of total lithium concentration. *NMR in biomedicine* 2013;26(9):1152-1157.
17. Sun Y, Schmidt NO, Schmidt K, Doshi S, Rubin JB, Mulkern RV, Carroll R, Ziu M, Erkmen K, Poussaint TY, Black P, Albert M, Burstein D, Kieran MW. Perfusion MRI of U87 brain tumors in a mouse model. *Magn Reson Med* 2004;51(5):893-899.
18. Grant AK, Vinogradov E, Wang XE, Lenkinski RE, Alsop DC. Perfusion Imaging with a Freely Diffusible Hyperpolarized Contrast Agent. *Magnetic Resonance in Medicine* 2011;66(3):746-755.
19. Mieville P, Ahuja P, Sarkar R, Jannin S, Vasos PR, Gerber-Lemaire S, Mishkovsky M, Comment A, Gruetter R, Ouari O, Tordo P, Bodenhausen G. Scavenging Free Radicals To Preserve Enhancement and Extend Relaxation Times in NMR using Dynamic Nuclear Polarization. *Angewandte Chemie-International Edition* 2010;49(35):6182-6185.
20. Cheng T, Mishkovsky M, Bastiaansen JAM, Ouari O, Hautle P, Tordo P, van den Brandt B, Comment A. Automated transfer and injection of hyperpolarized molecules with polarization measurement prior to in vivo NMR. *NMR in biomedicine* 2013;26(11):1582-1588.
21. Lumata L, Ratnakar SJ, Jindal A, Merritt M, Comment A, Malloy C, Sherry AD, Kovacs Z. BDPA: An Efficient Polarizing Agent for Fast Dissolution Dynamic Nuclear Polarization NMR Spectroscopy. *Chemistry* 2011;17(39):10825-10827.
22. Cade JF. Lithium salts in the treatment of psychotic excitement. *The Medical journal of Australia* 1949;2(10):349-352.
23. Thase ME, Denko T. Pharmacotherapy of mood disorders. *Annual review of clinical psychology* 2008;4:53-91.
24. Lee JH, Adler C, Norris M, Chu WJ, Fugate EM, Strakowski SM, Komoroski RA. 4-T 7Li 3D MR spectroscopy imaging in the brains of bipolar disorder subjects. *Magnetic Resonance in Medicine* 2012;68(2):363-368.
25. Nelson SJ, Kurhanewicz J, Vigneron DB, Larson PE, Harzstark AL, Ferrone M, van Criekinge M, Chang JW, Bok R, Park I, Reed G, Carvajal L, Small EJ, Munster P, Weinberg VK, Ardenkjaer-Larsen JH, Chen AP, Hurd RE, Odegardstuen LI, Robb FJ, Tropp J, Murray JA. Metabolic Imaging of Patients with Prostate Cancer Using Hyperpolarized [1-13C]Pyruvate. *Science translational medicine* 2013;5(198):198ra108.
26. Cheng T, Capozzi A, Takado Y, Balzan R, Comment A. Over 35% liquid-state C-13 polarization obtained via dissolution dynamic nuclear polarization at 7 T and 1 K using ubiquitous nitroxyl radicals. *Physical Chemistry Chemical Physics* 2013;15(48):20819-20822.
27. Comment A, van den Brandt B, Uffmann K, Kurdzesau F, Jannin S, Konter JA, Hautle P, Wenckebach WT, Gruetter R, van der Klink JJ. Design and performance of a DNP prepolarizer coupled to a rodent MRI scanner.

Concepts in Magnetic Resonance Part B: Magnetic Resonance Engineering
2007;31B(4):255-269.

Figure legends

Figure 1. Left: Schematic representation of the tube holder containing the three 10-mm glass tubes labeled from 1 to 3 and the surrounding 40-mm inner diameter coils. Tube #2 has thicker walls and served as reference to assess the relaxation time of each hyperpolarized ${}^6\text{Li}^+$ solution. Tubes #1 and #3 served for the relative measurements between whole and deoxygenated blood or plasma; **Right:** Cross section showing the arrangement of the three tubes inside the tube holder.

Figure 2. Top: Time evolution of the tomographic projection of the ${}^6\text{Li}$ signal measured following the simultaneous injection of hyperpolarized ${}^6\text{Li}^+$ solution into all three tubes. Projections were acquired along the horizontal axis perpendicular to the static field using a 2.5-ms 6-G/cm dephasing gradient and a 20-ms 1.5-G/cm acquisition gradient. **Bottom:** Integral of the projected ${}^6\text{Li}$ signal measured in tubes #1 to #3 as a function of time.

Figure 3. Mean relative change in ${}^6\text{Li}$ longitudinal relaxation time after deoxygenation of blood and plasma in both human and rat samples.

Table 1. Mean ${}^6\text{Li}$ longitudinal relaxation time measured in human and rat samples displayed with their standard deviation (SD) and relative standard deviation (RSD).

Table 2. Longitudinal relaxation time of ${}^6\text{Li}$ in various aqueous solutions. The measurements were performed on a 400 MHz high-resolution MR system (Bruker Biospin, Fällanden, Switzerland) using a saturation recovery protocol.

Table 3. Results of the oxygen gas analysis in blood and plasma samples. The measurements were performed using a COBAS[®] b 121 system (Roche Diagnostic GmbH, Mannheim, Germany).

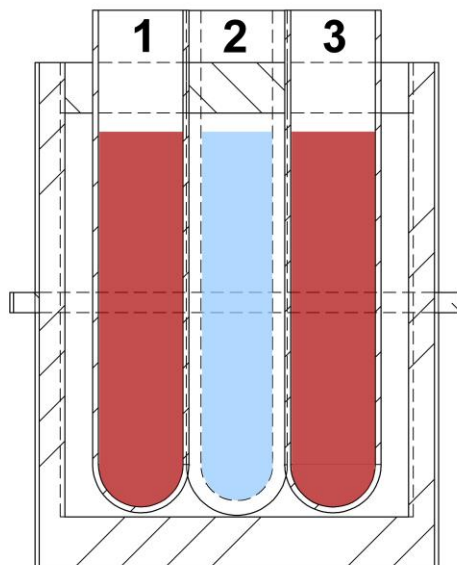
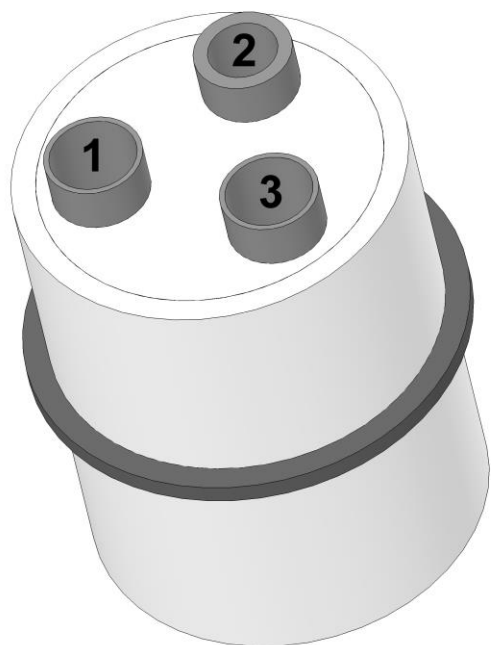
Figure 1

Figure 2

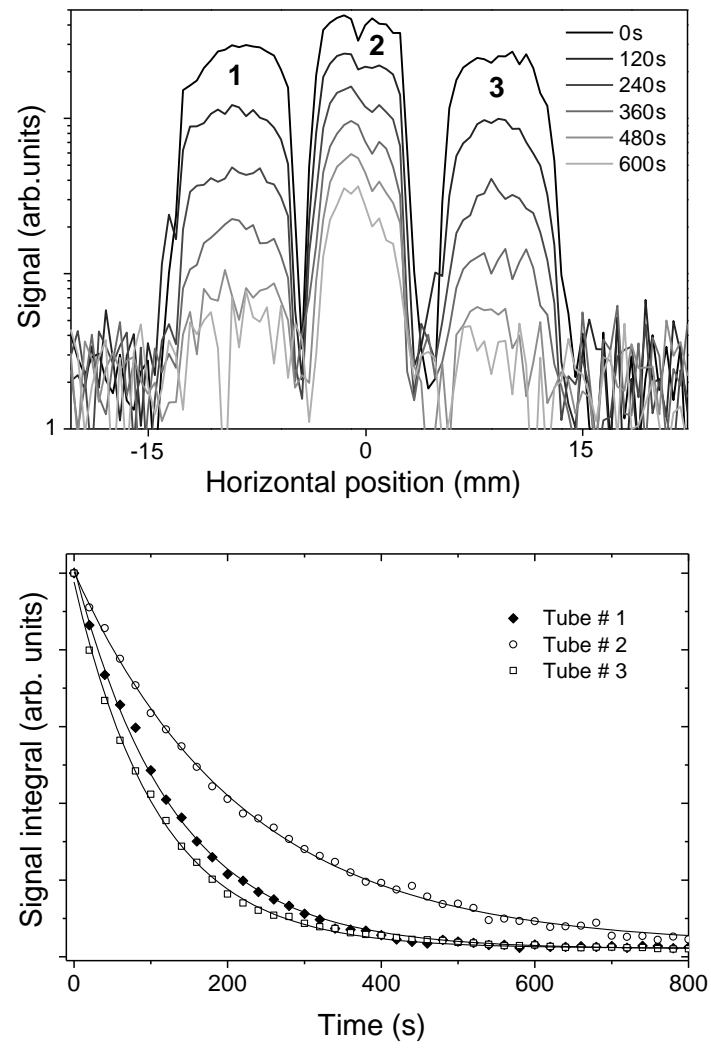


Figure 3

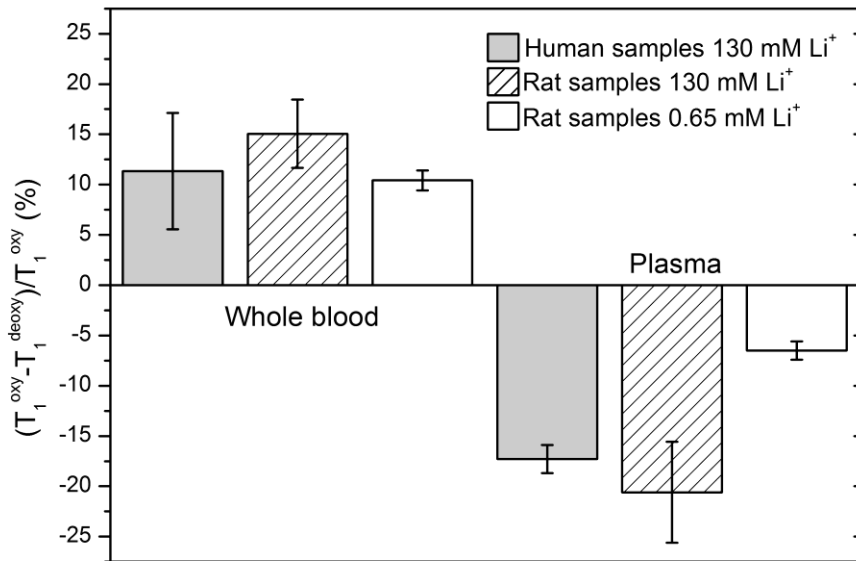


Table 1

Human samples (130 mM ^6Li , n = 3)	$^6\text{Li } T_1$ (s)	SD (s)	RSD (%)
Whole blood	177	31	17.5
Deoxygenated blood	157	28	17.8
Plasma	115	7	6.1
Deoxygenated plasma	135	10	7.4
Rat samples (130 mM ^6Li , n = 3)			
Whole blood	180	19	10.5
Deoxygenated blood	153	12	7.8
Plasma	103	7	6.8
Deoxygenated plasma	123	5	4.0
Rat samples (0.65 mM ^6Li , n = 4)			
Whole blood	161	2	1.2
Dexoxygenated blood	144	2	1.4
Plasma	137	4	2.9
Deoxygenated plasma	146	5	3.4

Table 2

Sample composition	${}^6\text{Li } T_1$ (s)
0.5 M ${}^6\text{LiCl}$ in pure D_2O	506 ± 10
0.5 M ${}^6\text{LiCl}$ in D_2O with 20 mM deuterated sodium ascorbate	401 ± 5
0.5 M ${}^6\text{LiCl}$ in D_2O with 20 mM sodium ascorbate	394 ± 5
Hyperpolarized ${}^6\text{LiCl}$ solution (n=6) (130 mM ${}^6\text{Li}$ in D_2O containing 1.2 mM ascorbate and 0.4 mM TEMPOL)	261 ± 5
Hyperpolarized ${}^6\text{LiCl}$ solution (n=8) (0.65 mM ${}^6\text{Li}$ in deuterated phosphate buffer containing 0.45 mM ascorbate and 0.015 mM TEMPOL)	413 ± 15

Table 3

Samples (n = 3)	PO₂ (mmHg)	SD (mmHg)	RSD (%)
Whole blood	45.9	0.6	1.3
Dexoygenated blood	43.5	0.5	1.1
Plasma	121.7	1.2	1.0
Deoxygenated plasma	77.9	13.4	17.2
Samples (n = 3)	SO₂ (%)	SD (%)	RSD (%)
Whole blood	76.9	0.3	0.4
Dexoygenated blood	75.4	0.7	0.9